JPET Fast Forward. Published on October 25, 2005 as DOI: 10.1124/jpet.105.094797

Presynaptic α_1 Adrenergic Receptors Differentially Regulate Synaptic Glutamate and GABA Release to Hypothalamic Presympathetic Neurons

Qian Chen, De-Pei Li, and Hui-Lin Pan

Department of Anesthesiology (Q.C., D.-P.L., H.-L.P.)

Department of Neural and Behavioral Sciences (H.-L.P.)

Pennsylvania State University College of Medicine

Hershey, PA 17033

Running Title: α_1 Adrenergic receptors and synaptic transmission

List of abbreviations:

γ-aminobutyric acid (GABA); Guanosine 5'-*O*-(2-thiodiphosphate) (GDP-β-S);

Miniature excitatory postsynaptic currents (mEPSCs);

N-methyl-D-aspartate (NMDA); DL-2-amino-5-phosphonovaleric acid (AP5);

Miniature inhibitory postsynaptic currents (mIPSCs);

Paraventricular nucleus (PVN); Spontaneous excitatory postsynaptic currents (sEPSCs);

Spontaneous inhibitory postsynaptic currents (sIPSCs);

Number of text pages: 32; Number of tables: 0; Number of figures: 7;

Number of words: Abstract, 235; Introduction, 462; Discussion, 1478

Number of references: 40

Address for correspondence:

Hui-Lin Pan, M.D., Ph.D.

Department of Anesthesiology, H187

Pennsylvania State University College of Medicine

500 University Drive

Hershey, PA 17033

Tel: (717) 531-8433; Fax: (717) 531-6221

E-mail: hpan@psu.edu

Abstract

The hypothalamic paraventricular nucleus (PVN) neurons that project to the spinal intermediolateral cell column and brainstem are important for the control of sympathetic outflow. Stimulation of α_1 adrenergic receptors in the PVN increases sympathetic outflow, but the cellular mechanisms remain unclear. In this study, we determined the role of α_1 adrenergic receptors in the regulation of glutamatergic and GABAergic synaptic inputs to spinally projecting PVN neurons. Whole-cell and cell-attached patch-clamp recordings were performed on retrogradely labeled PVN-spinal neurons in rat brain slices. Bath application of 50-100 μM phenylephrine, an α_1 adrenergic receptor agonist, significantly increased the frequency of spontaneous excitatory postsynaptic currents (EPSCs) in a concentration-dependent manner. This effect was blocked by the α_1 adrenergic receptor antagonists prazosin or corynanthine. Phenylephrine also significantly increased the frequency of miniature inhibitory postsynaptic currents (mIPSCs) but not the amplitude and decay constant of mEPSCs. Furthermore, activation of α_1 adrenergic receptors with phenylephrine or cirazoline significantly decreased the frequency of spontaneous EPSCs and mEPSCs, and this effect also was blocked by corynanthine. Additionally, 50 μM phenylephrine significantly increased the firing rate of 13 labeled PVN neurons from 3.16 ± 0.42 to 5.83 ± 0.65 Hz. However, phenylephrine failed to increase the firing of most labeled PVN neurons in the presence of $GABA_A$ and ionotropic glutamate receptor antagonists. Thus, these data suggest that activation of α_1 adrenergic receptors increases the excitability of PVN presympathetic neurons primarily through augmentation of glutamatergic tone and attenuation of GABAergic inputs.

Introduction

The paraventricular nucleus (PVN) of the hypothalamus is a major integrative site for autonomic and endocrine functions within the brain (Swanson and Sawchenko, 1983; de Wardener, 2001). The PVN consists of interneurons and different types of output neurons projecting to the pituitary and autonomic centers, such as the rostral ventrolateral medulla (RVLM), nucleus of solitary tract (NTS), as well as sympathetic preganglionic neurons in the intermediolateral cell column (IML) of the spinal cord (Shafton et al., 1998; Pyner and Coote, 2000). The PVN presympathetic neurons are important in the physiological control of blood pressure and sympathetic outflow. For example, bilateral inhibition of the PVN causes a large decrease in arterial blood pressure and suppression of sympathetic nerve activity (Allen, 2002; Zahner and Pan, 2005). The PVN presympathetic neurons may also contribute to long-term regulation of the sympathetic nervous system, especially during pathophysiological conditions such as heart failure and hypertension (Allen, 2002; Zhang et al., 2002a; Zhang et al., 2002b).

The tonic activity of PVN neurons is regulated by various excitatory and inhibitory neurotransmitters and neuromodulators, including glutamate, GABA, angiotensin II, nitric oxide, and catecholamines (Decavel and van den Pol, 1992; Tasker and Dudek, 1993; Li et al., 2002; Li et al., 2003). A majority of GABAergic and glutamatergic inputs to the PVN neurons are derived from the suprachiasmatic nucleus, subfornical organ, and other brain regions (Bains and Ferguson, 1995; Cui et al., 2001). Also, there exist considerable GABAergic and glutamatergic interneurons in the PVN (Decavel and van den Pol, 1992; Tasker and Dudek, 1993). Many important neuromodulators, such as nitric oxide and angiotensin II, can regulate

PVN presympathetic neurons by indirect effects on GABAergic transmission (Li et al., 2002; Li et al., 2003).

The PVN neurons receive dense noradrenergic projections from the brainstem, especially A1, A2 and A6 (locus coeruleus) noradrenergic cell groups (Swanson and Sawchenko, 1983; Cunningham and Sawchenko, 1988) and adrenergic inputs from the C1, C2, and C3 neurons in the rostral medulla (Cunningham et al., 1990). Furthermore, both α_1 and α_2 adrenergic receptors are present in the PVN (Cummings and Seybold, 1988). Microinjection of norepinephrine into the PVN raises the blood pressure in rats, and this effect is due in part to the release of arginine vasopressin (Harland et al., 1989). We recently found that stimulation of α_2 adrenergic receptors attenuates GABAergic, but not glutamatergic, inputs to spinally projecting PVN neurons (Li et al., 2005). Because the function of α_1 adrenergic receptors has not been specifically studied in PVN output neurons with known projections, the role of α_1 receptors in the regulation of the excitability of PVN presympathetic neurons remains unclear. In this study, using *in vivo* retrograde labeling and *in vitro* brain slice recordings, we determined the role of α_1 adrenergic receptors in the control of glutamatergic and GABAergic inputs to spinally projecting PVN neurons.

METHODS

Retrograde labeling of spinally projecting PVN neurons

Male Sprague-Dawley rats (3-5 wk old, Harlan, Indianapolis, IN) were used for this study. The surgical preparations and experimental protocols were approved by the Animal Care and Use Committee of the Pennsylvania State University College of Medicine and conformed to the National Institutes of Health guidelines on the ethical use of animals. All efforts were made to minimize both the suffering and number of animals used. The dorsal laminectomy was performed at the T_2-T_4 level of the spinal cord under halothane (2% in O_2) anesthesia. A rhodamine-labeled fluorescence microsphere suspension (FluoSpheres, 0.04 μm, Molecular Probes, Eugene, OR) was pressure-injected (Nanojector II, Drummond Scientific Company, Broomall, PA) bilaterally into the IML region of the spinal cord in three or four separate 50-nl injections using a glass micropipette (tip diameter, 20-30 μm). Using a manipulator, the pipette was positioned at about 500 μm from the midline and 500 μm below the dorsal surface (Li et al., 2002; Li et al., 2003). After injection, animals were returned to their cages for 3-10 days and inspected daily for motor activity, signs of infection, as well as food and water intake to assess the health status of the animals. Because the fluorescence tracer can reach the PVN within 48 hours and is retained in labeled neurons for more than 10 days, the recording on the brain slice (one rat/day) was done 3-10 days after the tracer injection. In our previous studies, we found no difference of EPSCs and IPSCs recorded over a period of 3-10 days in these animals (Li et al., 2002; Li et al., 2003).

Slice preparations

After 3-10 days, the brain of the FluoSphere-injected rats was quickly removed under halothane anesthesia and placed in ice-cold artificial cerebral spinal fluid (aCSF) perfusion solution containing (in mM): 124.0 NaCl, 3.0 KCl, 1.3 $MgSO_4$, 2.4 $CaCl_2$, 1.4 NaH_2PO_4, 10.0 glucose, and 26.0 $NaHCO_3$ saturated with 95% O_2-5% CO_2 for 1-2 min. A higher glucose concentration was used to better preserve the viability of neurons in brain slices. A brain block containing the hypothalamus was trimmed and glued onto the stage of the vibratome (Technical Product International, St. Louis, MO), as we described previously (Li et al., 2003; Li et al., 2005). Coronal slices (300 μm in thickness) containing the PVN were cut in the ice-cold aCSF. Before recording, the slices were incubated in the aCSF continuously gassed with 95% O_2-5% CO_2 at 34°C for at least 1 hour.

Recordings of postsynaptic currents and action currents of PVN neurons

The slice was placed in a glass-bottomed chamber (Warner Instrument, Hamden, CT) and fixed with a grid of parallel nylon threads supported by a U-shaped stainless steel weight. The aCSF was perfused at 3.0 ml/min at 34°C maintained by an in-line solution heater and a temperature controller (model TC-324, Warner Instruments). Whole-cell voltage-clamp recordings were performed to record the postsynaptic currents of the labeled PVN, as we described previously (Li et al., 2002; Li et al., 2003). The recording pipette was pulled using borosilicate capillaries (1.2 mm OD, 0.86 mm ID; World Precision Instruments, Sarasota, FL). The resistance of the pipette was 5-7 MΩ when it was filled with the pipette solution. The PVN is easily distinguishable under the microscope since it has a higher density of somata passing

more light than surrounding tissues. The fluorescence-labeled neurons located in the medial one-third of the PVN area between the third ventricle and the fornix were selected for recording using a combination of epifluorescence illumination and differential interference contrast optics on a fixed-stage upright microscope (BX51WI, Olympus, Tokyo, Japan). The labeled neuron was briefly identified with the aid of epifluorescence illumination. After forming a tight GΩ seal, a brief negative pressure was used to get the whole-cell configuration. Recordings of postsynaptic currents began 5 min later when the current reached a steady state. Signals were processed with an Axopatch 700B amplifier (Axon Instruments, Foster City, CA), filtered at 1-2 kHz, digitized at 20 kHz using DigiData 1322 (Axon Instruments), and saved to a hard drive of a computer. A liquid junction potential of -15.3 mV (for the potassium gluconate pipette solution) was corrected. To record EPSCs, the internal solution contained (in mM): 130.0 potassium gluconate, 2.0 $MgCl_2$, 0.1 $CaCl_2$, 1.1 EGTA, 10.0 HEPES, 2.0 Na_2ATP, 0.3 Na_2GTP, adjusted to pH 7.25 with 1 M KOH (280-300 mOsm). Bicuculline (20 μM) was applied continuously to block the IPSCs at the holding potential of -70 mV. For recording of IPSCs, 130.0 mM potassium gluconate was replaced by 110.0 mM Cs_2SO_4 in the pipette solution, and 20 μM 6-cyano-7-nitroquinoxaline-2,3-dione (CNQX, a glutamate non-NMDA receptor antagonist) was used to block EPSCs at the holding potential of 0 mV. The mEPSCs and mIPSCs were recorded in the presence of 1 μM tetrodotoxin (TTX). To block the possible postsynaptic action mediated by G proteins coupled to adrenergic receptors, a general G protein inhibitor, guanosine 5'-*O*-(2-thiodiphosphate) (GDP-β-s, 1 mM), was added into the pipette solution during the whole-cell recording. A sodium channel blocker, lidocaine N-ethyl bromide (QX-314, 10 mM), was included in the pipette solution to suppress the action potential

generation in whole-cell voltage-clamp protocols. The mEPSCs recorded in the presence of TTX represent the quantal release of glutamate (independent of the action potential), while sEPSCs reflect action potential-triggered and action potential-independent spontaneous glutamate release.

Cell-attached recordings were performed to examine the drug effect on the firing activity of PVN neurons. In these experiments, action currents were measured in the cell-attached configuration as a capacitive current that charges the membrane (Charles and Hales, 1995). The advantage of measuring action currents in the cell-attached configuration, as compared with whole-cell recording of action potentials, is that the intracellular contents of a cell are not disturbed while action currents are monitored. The patch was voltage-clamped to 0 mV relative to the bath potential. The capacitive current that is measured when the cell fires an action potential appears as a brief spike. Data collection was terminated if the seal resistance fell below 1 GΩ.

Phenylephrine, cirazoline, prazosin, CNQX disodium, bicuculline methiodide, AP5, and GDP-β-s were purchased from Sigma (St. Louis, MO), TTX and QX-314 from Alomone Labs (Jerusalem, Israel), and corynanthine hydrochloride from Tocris (Ellisville, MO). Prazosin and corynanthine were initially dissolved in DMSO to make the stock solution before being diluted in aCSF. Other drugs and agents, including phenylephrine, cirazoline, CNQX, bicuculline, and AP5, were dissolved in aCSF. All the drugs and solutions were freshly prepared before the experiment and delivered using syringe pumps. The reported selectivity value (α_1/α_2 adrenergic receptors) for corynanthine, prazosin, and cirazoline is 100, 1000-5000, and 50-100, respectively (Cavero et al., 1982; Doxey et al., 1984; Angel et al., 1995; Ireland et al., 1997).

Data analysis

Data are presented as means ± SEM. The amplitude and frequency of EPSCs and IPSCs, and the firing activity were analyzed off-line using a peak detection program (MiniAnalysis; Synaptosoft, Leonia, NJ). Detection of events was accomplished by setting a threshold above the noise level. The representative tracings were extracted from original recordings over a 3 min period during control, during drug application, and washout. The mean amplitude and frequency of sEPSCS/sIPSCS and mEPSCs/mIPSCs were first determined for each recording and then averaged together according to the experimental group. The cumulative probability of the amplitude and inter-event interval of EPSCs and IPSCs was compared using the Komogorov-Smirnov test, which estimates the probability that two cumulative distributions are similar. At least 100 EPSCs and 100 IPSCs were used in each analysis. The cumulative probability is a function used to analyze a random (discrete or continuous) variable. Specifically, cumulative probability plots rank the data in a simulation from the highest to the lowest value, and graph each point with its corresponding percentile (1 = 100%). The sEPSCS/sIPSCS and mEPSCs/mIPSCs recorded in this study are random events. Thus, to compare the drug effect on these variables, it is appropriate to analyze these data using cumulative probability. Neurons were considered to be responsive to drugs if the frequency of EPSCs or IPSCs was altered > 20%. The decay phase of mIPSCs and mEPSCs were obtained by fitting the decaying phase of mIPSCs and mEPSCs using one or two exponential functions based on the curve fitting R^2 values. The effect of drugs on the amplitude and frequency of EPSCs and IPSCs was determined by the nonparametric Wilcoxon signed rank test or

nonparametric ANOVA (Kruskal-Wallis) with Dunn's post hoc test. $P < 0.05$ was considered to be statistically significant.

Results

Whole-cell voltage-clamp recordings were performed on a total of 137 labeled PVN cells. The spinal cord around the level of T_2-T_4 was taken out after killing the rat and sectioned into 30 μm slices. The slices were viewed under the fluorescence microscope to verify the injection and diffusion sites of the tracer, as we described previously (Li et al., 2002; Li et al., 2003). These sites were largely located in and around the IML of the spinal cord. The labeled PVN neurons displayed a membrane potential between -55 and -75 mV and an input resistance in a range of 500-800 MΩ.

Stimulation of α_1 adrenergic receptors increases the frequency of sEPSCs and mEPSCs

To determine the role of presynaptic α_1 adrenergic receptors in the regulation of glutamatergic synaptic inputs to spinally projecting PVN neurons, we first tested the effect of the α_1 adrenergic receptor agonist phenylephrine (Han et al., 2002) on sEPSCs in labeled PVN neurons. At 1 and 10 μM, phenylephrine did not significantly change the frequency of sEPSCs. Bath application of phenylephrine (50-100 μM) significantly increased the frequency of sEPSCs in 19 of 25 (76%) labeled PVN neurons, but did not significantly alter the amplitude of sEPSCs (Fig. 1). The increase in the frequency of sEPSCs occurred approximately 5.6 ± 4.2 min after perfusion of phenylephrine into the recording chamber. The frequency of sEPSCs returned to ~86% of the control level 20-30 min after washout of the drug. The sEPSCs were completely

blocked by 20 μM CNQX (Fig. 1A).

Phenylephrine (50-100 μM) did not significantly increase the frequency of sEPSCs (from 9.52 ± 2.35 to 9.69 ± 2.34 Hz at 100 μM) in another 6 cells. Notably, the baseline frequency of sEPSCs of these 6 non-responsive cells to phenylephrine varied from 1.23 to 15.14 Hz. For those cells with the frequency of sEPSCs less than 3 Hz, phenylephrine also failed to alter the EPSC frequency. Thus, lack of response of sEPSCs to phenylephrine in these cells is less likely due to the high baseline frequency of sEPSCs.

To further examine if the effect of phenylephrine is mediated through α_1 adrenergic receptors, the α_1 adrenergic receptor antagonist, corynanthine (100 μM) or prazosin (20 μM), was perfused 3-4 minutes before bath application of 50 μM phenylephrine. The concentrations of these α_1 adrenergic receptor antagonists have been determined in previous studies (Medgett and Langer, 1984; Han et al., 2002; Li et al., 2005). Each antagonist alone did not significantly change the frequency of sEPSCs. However, corynanthine or prazosin alone completely blocked the effect of phenylephrine on the frequency of sEPSCs in 20 labeled cells (Fig. 2).

To determine if phenylephrine increases synaptic glutamate release by acting at presynaptic terminals or a presumed somatodendritic site, we examined the effect of phenylephrine on mEPSCs in the presence of 1 μM TTX. In 15 labeled cells tested, 50 μM phenylephrine significantly increased the frequency of sEPSCs of 13 cells from 6.46 ± 1.26 to 12.70 ± 2.14 Hz. It did not affect the frequency of sEPSCs in another 2 cells (from 3.45 to 3.86 Hz in one cell, and from 4.73 to 5.26 Hz in the other). Phenylephrine also significantly increased the frequency of mEPSCs from 6.03 ± 1.35 to 9.77 ± 2.09 Hz in all 13 cells (Fig. 3D), but had no significant effects on the amplitude and decay constant of mEPSCs (Fig. 3, B and C).

Activation of α_1 adrenergic receptors decreases the frequency of sIPSCs and mIPSCs

We next tested the effects of phenylephrine on GABAergic sIPSCs and mIPSCs. In 13 of 15 (87%) cells tested, phenylephrine (50-100 μM) reversibly decreased the frequency of sIPSCs in a concentration-dependent manner (Fig. 4A-C). In another 2 cells, 100 μM phenylephrine did not alter the frequency of sIPSCs (from 6.84 to 6.93 Hz in one cell, and from 2.12 to 2.45 Hz in another one). Phenylephrine did not significantly affect sIPSCs at 1 and 10 μM. At 50 and 100 μM, phenylephrine caused a significant decrease in the frequency of sIPSCs (from 3.23 ± 0.43 to 1.89 ± 0.23 Hz at 50 μM and 1.71 ± 0.19 Hz at 100 μM, n = 13, both $P < 0.05$, Fig. 4A-C). However, phenylephrine did not significantly alter the amplitude of sIPSCs. Bath application of 20 μM bicuculline completely blocked sIPSCs (Fig. 4A).

Phenylephrine produced a different effect on synaptic GABA release in the PVN in the present and previous study (Han et al, 2002). To further determine the effect of α_1 adrenergic receptor activation on the frequency of sIPSCs, cirazoline, another α_1 adrenergic receptor agonist, was used. The concentration of cirazoline has been examined in the previous study (Pudovkina et al., 2001). In another 7 labeled PVN cells examined, bath application of 50 to 100 μM cirazoline also caused a significant decrease in the frequency of sIPSCs (Fig. 4D).

To ensure that the effect of phenylephrine on sIPSCs is mediated by α_1 adrenergic receptors, corynanthine (100 μM), an α_1 receptor antagonist, was applied for 3-4 minutes before perfusion of 50 μM phenylephrine. Corynanthine alone did not significantly change the frequency of sIPSCs, but it completely abolished the phenylephrine-induced decrease in the frequency of sIPSCs in all 9 cells tested (Fig. 5).

Furthermore, in 13 of 18 (72%) cells tested, 50 μM phenylephrine significantly decreased the frequency of mIPSCs from 2.80 ± 0.55 to 1.80 ± 0.39 Hz. However, 50 μM phenylephrine had no significant effect on the amplitude and decay constant of mIPSCs in these 13 labeled cells (Fig. 6). Phenylephrine did not significantly change the frequency of mIPSCs (from 3.17 ± 0.67 to 2.71 ± 0.55 Hz) in another 5 cells.

Effect of phenylephrine on the firing activity of labeled PVN neurons in the presence of synaptic blockade

Cell-attached recordings were performed to record the firing activity of labeled PVN neurons. In 13 of 19 (68%) cells, 50 μM phenylephrine significantly increased the firing from 3.16 ± 0.42 to 5.83 ± 0.65 Hz (n = 13, Fig. 7, A and B). To determine if the presynaptic action of phenylephrine on GABA/glutamate release plays a role in the excitatory effect of phenylephrine on the firing, the $GABA_A$ receptor antagonist (20 μM bicuculline methiodide) and the glutamate non-NMDA antagonist (20 μM CNQX) and the NMDA antagonist (20 μM AP5) were applied together for 3-4 minutes to block the GABAergic and glutamatergic inputs. Bath application of these antagonists alone did not significantly change the firing rate of labeled PVN neurons. In the presence of synaptic blockade, 50 μM phenylephrine failed to increase the firing rate in 11 of 13 (85%) cells (Fig. 7, A and B). In another 2 cells, 50 μM phenylephrine still increased the firing rate (from 3.64 to 6.02 Hz in one cell, and from 12.20 to 18.88 Hz in the other).

Phenylephrine had no significant effect on another 6 cells (from 6.15 ± 1.04 to 6.96 ± 1.23 Hz). Notably, the baseline frequency of the firing activity of these 6 non-responsive cells to

50 μM phenylephrine ranged from 2.79 to 10.29 Hz. For those cells with the firing rate less than 4 Hz, phenylephrine also failed to alter their firing activity. Therefore, lack of response of the firing activity to phenylephrine in these cells is less likely due to the high baseline firing rate.

In addition to blocking $GABA_A$ receptors, bicuculline methiodide may increase the firing activity of PVN neurons through its effect on small conductance Ca^{2+}-activated K^+ channels (SK channels) (Khawaled et al., 1999). Therefore, we determined the effect of apamin, a specific blocker of SK channels, on the firing activity of labeled PVN neurons. Bath application of 20 μM bicuculline methiodide significantly increased the firing rate of 8 labeled PVN neurons. However, 100 nM apamin had no significant effect on the firing rate of these 8 PVN neurons (Fig. 7C). At 500 nM, apamin also failed to alter the firing activity of these neurons (Fig. 7C).

Discussion

In this study, we used retrograde labeling and whole-cell recording techniques in brain slices to investigate the role of α_1 adrenergic receptors in the regulation of synaptic inputs to PVN-spinal projection neurons. We found that phenylephrine significantly increased the frequency of glutamatergic sEPSCs and mEPSCs. On the other hand, phenylephrine significantly decreased the frequency of GABAergic sIPSCs and mIPSCs. These presynaptic effects of phenylephrine on glutamate and GABA release were blocked by specific α_1 adrenergic receptor antagonists. Furthermore, phenylephrine failed to increase the firing of labeled PVN neurons in the presence of $GABA_A$ and ionotropic glutamate receptor antagonists in most of the cells tested. Therefore, our results provide important new evidence showing that activation of presynaptic α_1 adrenergic receptors increases glutamatergic, but reduces GABAergic inputs, to augment the excitability of PVN presympathetic neurons.

The hypothalamic PVN neurons are important for autonomic regulation mainly through its projections to the RVLM, NTS, and IML of the spinal cord. The PVN receives dense catecholaminergic afferents from the brainstem neurons, including the A1, A2, A6 noradrenergic cell groups (Swanson and Sawchenko, 1983; Cunningham and Sawchenko, 1988) and C1, C2, C3 adrenergic neurons in the rostral medulla (Cunningham et al., 1990). Receptor binding studies have shown that α_1 and α_2 adrenergic receptors are present in the PVN (Cummings and Seybold, 1988). Many studies have shown that α_1 adrenergic receptors in the PVN play an important role in the regulation of neuroendocrine function. For instance, norepinephrine increases corticotrophin-releasing hormone release through α_1 adrenergic

receptors (Plotsky, 1987). Microinjection of norepinephrine into the PVN causes an increase in blood pressure through α_1 adrenergic receptors (Harland et al., 1989). Increased release of norepinephrine in the PVN also may stimulate the secretion of vasopressin through α_1 adrenergic receptors to increase blood pressure (Bealer and Abell, 1995). However, the cellular and synaptic mechanisms responsible for the effects of norepinephrine and α_1 agonists on PVN presympathetic neurons are not clear. Therefore, in this study we used retrograde labeling to identify the PVN-spinal projection neurons, and investigated the role of α_1 adrenergic receptors in regulation of glutamatergic and GABAergic synaptic inputs to labeled PVN neurons.

Glutamate is considered the dominant excitatory neurotransmitter in the PVN (Decavel and van den Pol, 1992). Microinjection of glutamate into the PVN increases renal sympathetic activity (Kannan et al., 1989). The local glutamatergic synaptic inputs may originate from the dorsomedial hypothalamus and perifornical neurons. Also, the PVN neurons in the brain slice receive glutamatergic projections from the caudal bed nucleus, the subparaventricular zone, the suprachiasmatic nucleus, the lateral hypothalamus, and the rostral zona incerta (Bains and Ferguson, 1995; Cui et al., 2001). We found that phenylephrine significantly increased the frequency of sEPSCs of labeled PVN neurons. This effect was blocked by either prazosin aor corynanthine, the α_1 adrenergic receptor antagonist. Phenylephrine also increased the frequency of mEPSCs but did not change the amplitude and decay constant of mEPSCs, suggesting that α_1 adrenergic receptors are located at the presynaptic terminals. Although previous studies have shown that norepinephrine stimulates glutamatergic synaptic inputs to PVN magnocellular and parvocellular neurons through presynaptic α_1 adrenergic receptors (Daftary et al., 1998; Daftary et al., 2000; Boudaba et al., 2003), the potential function and projections of these neurons are

not defined. Therefore, our results provide new information that activation of presynaptic α_1 adrenergic receptors enhances the glutamatergic synaptic inputs to PVN-spinal output neurons to increase sympathetic outflow.

Data from our study strongly suggest that activation of α_1 adrenergic receptors on presynaptic terminals reduces synaptic GABA release to PVN presympathetic neurons. The local synaptic inputs to PVN neurons are primarily GABAergic (Decavel and van den Pol, 1992; Tasker and Dudek, 1993). Unlike the glutamatergic input, the PVN GABAergic system tonically inhibits the PVN presympathetic neurons (Li et al., 2002; Li et al., 2003; Li et al., 2005) and the sympathetic outflow (Martin and Haywood, 1993). In this study, we found that two structurally dissimilar α_1 adrenergic receptor agonists, phenylephrine and cirazoline, both significantly decreased the frequency of GABAergic sIPSCs. This effect was completely blocked by the α_1 adrenergic receptor antagonist corynanthine. Also, phenylephrine significantly decreased the frequency of mIPSCs but did not affect the amplitude and decay constant of mIPSCs, suggesting that presynaptic α_1 adrenergic receptors alters the release probability of GABA-filled vesicles. Notably, in unlabeled PVN type II (parvocellular) neurons in brain slices, norepinephrine both increases and decreases the IPSC frequency, and norepinephrine-induced decreases in IPSC frequency was blocked by α_{2A}, but not α_1, receptor antagonists (Chong et al., 2004). Also, a previous study reports that norepinephrine increases the frequency of sIPSCs of some PVN neurons through α_1 adrenergic receptors, and this effect is sensitive to TTX (Han et al., 2002). This discrepancy may be related to our focus on spinally projecting PVN neurons, while the types of PVN neurons (i.e., interneurons vs. output neurons) are not clarified in the study by Han et al (2002). These results suggest a possible anatomical

and functional segregation of norepinephrine inputs among different parvocellular PVN subpopulations. Data from our study strongly suggest that activation of α_1 adrenergic receptors on presynaptic terminals reduces synaptic GABA release to PVN presympathetic neurons. We have shown that stimulation of α_2 adrenergic receptors decreases GABAergic (but not glutamatergic) inputs to PVN-spinal neurons (Li et al., 2005). In a given PVN neuron, the net presynaptic effect of norepinephrine on the GABA release depends on the presence and relative density of α_1 and α_2 adrenergic receptors on the presynaptic nerve terminals.

The excitability of PVN neurons critically depends on the balance between the excitatory and inhibitory inputs. Glutamate and GABA are the predominant excitatory and inhibitory neurotransmitters, respectively, in the PVN. We therefore further determined the contribution of the presynaptic effect of phenylephrine to the regulation of the firing activity of PVN-spinal output neurons. We found that combined treatment with bicuculline and CNQX/AP5 had no significant effect on basal discharges, suggesting that GABAergic and glutamatergic tone are in an effective balance. Phenylephrine significantly increased the firing of most labeled PVN neurons. However, the stimulatory effect of phenylephrine on most PVN neurons was abolished when the glutamatergic and GABAergic synaptic inputs were removed. This finding suggests that the excitatory effect of phenylephrine largely depends on its presynaptic effects on GABAergic and glutamatergic inputs to labeled PVN neurons. Bicuculline microinjection into the PVN of intact rats fails to increase sympathetic nerve activity if ionotropic glutamate receptors have been previously blocked (Chen et al., 2003). This suggests that local disinhibition of neurons following bicuculline injection may potentiate glutamate release and the increase in the firing activity of PVN neurons may be dependent on this process. Thus, it is

possible that norepinephrine-induced inhibition of IPSCs is required for the increase in glutamatergic EPSCs. Since may increase the firing activity of PVN neurons through its effect on small conductance Ca^{2+}-activated K^+ channels (SK channels) (Khawaled et al., 1999), we determined the effect of apamin, a specific blocker of SK channels, on the firing activity of labeled PVN neurons. We found that bicuculline methiodide, but not apamin, significantly increased the firing activity of labeled PVN neurons. Therefore, it is less likely that SK channels are involved in the excitatory effect of bicuculline on spinally projecting PVN neurons. The α_1 adrenergic receptors may affect other neurotransmitters and neuromodulators to regulate the activity of PVN neurons. In this regard, it has been shown that norepinephrine increases the nitric oxide synthase in PVN magnocellular neurons (Grange-Messent et al., 2004). However, the effect of activation of α_1 adrenergic receptors on the release of catecholamines and adenosine to PVN presympathetic neurons has not been demonstrated. Because some spinally projecting PVN neurons also send collaterals to the RVLM (Pyner and Coote, 2000), the increase in the firing activity of these PVN neurons by the α_1 adrenergic receptors could possibly excite the presympathetic neurons in the RVLM. Hence, stimulation of α_1 adrenergic receptors in the PVN can activate both PVN-IML- and PVN-RVLM-IML-descending pathways and could cooperatively augment the sympathetic outflow to increase the blood pressure (Harland et al., 1989).

In the PVN, three α_1 adrenergic receptor subtypes (α_{1A}, α_{1B}, and α_{1D}) have been identified by immunohistochemistry and *in situ* hybridization techniques (Domyancic and Morilak, 1997; Acosta-Martinez et al., 1999; Day et al., 1999; Sands and Morilak, 1999). The α_{1A} mRNA is mainly detected in the lateral magnocellular region in a lower expression level. The α_{1D} mRNA

is primarily in the PVN magnocellular and parvocellular subnuclei, while the α_{1B} immunoreactivity is higher in the magnocellular PVN division than in the parvocellular region (Domyancic and Morilak, 1997; Acosta-Martinez et al., 1999; Sands and Morilak, 1999). It is not clear why stimulation of α_1 adrenergic receptors increases synaptic glutamate release but decreases GABA release to spinally projecting PVN neurons. This may be due to that different subtypes of α_1 receptors and signaling pathways are present at the glutamatergic and GABAergic synaptic terminals. For example, the effect of α_{1A} is coupled to pertussis toxin (PTX)-sensitive G proteins, but both α_{1B} and α_{1D} receptors are coupled to PTX-insensitive G proteins in CHO cells (Perez et al., 1993). However, highly specific antagonists and agonists for these α_1 receptor subtypes are not available at this time to further define the function of α_1 receptor subtypes. In this study, the firing activity of 2 of 13 cells was still increased by phenylephrine after the synaptic blockade. This suggests that the excitability of a few PVN-spinal projection neurons is probably controlled by postsynaptic α_1 adrenergic receptors.

In summary, the present study provides new information that stimulation of presynaptic α_1 adrenergic receptors increases the firing of PVN projection neurons through attenuation of tonic GABAergic inhibition and potentiation of excitatory glutamatergic inputs. It has been shown that norepinephrine release in the PVN is increased in hypertensive rats (Qualy and Westfall, 1988; Woo et al., 1993). Furthermore, the firing rate of PVN neurons and the basal norepinephrine level in the PVN are elevated during heart failure (Arabia et al., 2002; Zhang et al., 2002b). Further studies are warranted to determine the role of α_1 adrenergic receptors in the PVN in the regulation of sympathetic outflow under these pathophysiological conditions.

REFERENCES

Acosta-Martinez M, Fiber JM, Brown RD and Etgen AM (1999) Localization of alpha1B-adrenergic receptor in female rat brain regions involved in stress and neuroendocrine function. *Neurochem Int* **35**:383-391.

Allen AM (2002) Inhibition of the hypothalamic paraventricular nucleus in spontaneously hypertensive rats dramatically reduces sympathetic vasomotor tone. *Hypertension* **39**:275-280.

Angel I, Le Rouzic M, Pimoule C, Graham D and Arbilla S (1995) [3H]cirazoline as a tool for the characterization of imidazoline sites. *Ann N Y Acad Sci* **763**:112-124.

Arabia AM, Catapano L, Storini C, Perego C, De Luigi A, Head GA and De Simoni MG (2002) Impaired central stress-induced release of noradrenaline in rats with heart failure: a microdialysis study. *Neuroscience* **114**:591-599.

Bains JS and Ferguson AV (1995) Paraventricular nucleus neurons projecting to the spinal cord receive excitatory input from the subfornical organ. *Am J Physiol* **268**:R625-633.

Bealer SL and Abell SO (1995) Paraventricular nucleus histamine increases blood pressure by adrenoreceptor stimulation of vasopressin release. *Am J Physiol* **269**:H80-85.

Boudaba C, Di S and Tasker JG (2003) Presynaptic noradrenergic regulation of glutamate inputs to hypothalamic magnocellular neurones. *J Neuroendocrinol* **15**:803-810.

Cavero I, Lefevre-Borg F, Roach AG, Gomeni R and Scatton B (1982) Functional and biochemical evidence for the lack of cardiac presynaptic alpha-2 adrenoceptor stimulant properties of cirazoline (LD 3098), a potent alpha-1 adrenoceptor agonist in dogs and

rats. *J Pharmacol Exp Ther* **223**:241-250.

Charles AC and Hales TG (1995) Mechanisms of spontaneous calcium oscillations and action potentials in immortalized hypothalamic (GT1-7) neurons. *J Neurophysiol* **73**:56-64.

Chen QH, Haywood JR and Toney GM (2003) Sympathoexcitation by PVN-injected bicuculline requires activation of excitatory amino acid receptors. *Hypertension* **42**:725-731.

Chong W, Li LH, Lee K, Lee MH, Park JB and Ryu PD (2004) Subtypes of alpha1- and alpha2-adrenoceptors mediating noradrenergic modulation of spontaneous inhibitory postsynaptic currents in the hypothalamic paraventricular nucleus. *J Neuroendocrinol* **16**:450-457.

Cui LN, Coderre E and Renaud LP (2001) Glutamate and GABA mediate suprachiasmatic nucleus inputs to spinal-projecting paraventricular neurons. *Am J Physiol Regul Integr Comp Physiol* **281**:R1283-1289.

Cummings S and Seybold V (1988) Relationship of alpha-1- and alpha-2-adrenergic-binding sites to regions of the paraventricular nucleus of the hypothalamus containing corticotropin-releasing factor and vasopressin neurons. *Neuroendocrinology* **47**:523-532.

Cunningham ET, Jr., Bohn MC and Sawchenko PE (1990) Organization of adrenergic inputs to the paraventricular and supraoptic nuclei of the hypothalamus in the rat. *J Comp Neurol* **292**:651-667.

Cunningham ET, Jr. and Sawchenko PE (1988) Anatomical specificity of noradrenergic inputs to the paraventricular and supraoptic nuclei of the rat hypothalamus. *J Comp Neurol* **274**:60-76.

Daftary SS, Boudaba C, Szabo K and Tasker JG (1998) Noradrenergic excitation of

magnocellular neurons in the rat hypothalamic paraventricular nucleus via intranuclear glutamatergic circuits. *J Neurosci* **18**:10619-10628.

Daftary SS, Boudaba C and Tasker JG (2000) Noradrenergic regulation of parvocellular neurons in the rat hypothalamic paraventricular nucleus. *Neuroscience* **96**:743-751.

Day HE, Campeau S, Watson SJ, Jr. and Akil H (1999) Expression of alpha(1b) adrenoceptor mRNA in corticotropin-releasing hormone-containing cells of the rat hypothalamus and its regulation by corticosterone. *J Neurosci* **19**:10098-10106.

de Wardener HE (2001) The hypothalamus and hypertension. *Physiol Rev* **81**:1599-1658.

Decavel C and van den Pol AN (1992) Converging GABA- and glutamate-immunoreactive axons make synaptic contact with identified hypothalamic neurosecretory neurons. *J Comp Neurol* **316**:104-116.

Domyancic AV and Morilak DA (1997) Distribution of alpha1A adrenergic receptor mRNA in the rat brain visualized by in situ hybridization. *J Comp Neurol* **386**:358-378.

Doxey JC, Lane AC, Roach AG and Virdee NK (1984) Comparison of the alpha-adrenoceptor antagonist profiles of idazoxan (RX 781094), yohimbine, rauwolscine and corynanthine. *Naunyn Schmiedebergs Arch Pharmacol* **325**:136-144.

Grange-Messent V, Raison D, Dugas B and Calas A (2004) Noradrenaline up-regulates the neuronal and the inducible nitric oxide synthase isoforms in magnocellular neurons of rat brain slices. *J Neurosci Res* **78**:683-690.

Han SK, Chong W, Li LH, Lee IS, Murase K and Ryu PD (2002) Noradrenaline excites and inhibits GABAergic transmission in parvocellular neurons of rat hypothalamic paraventricular nucleus. *J Neurophysiol* **87**:2287-2296.

Harland D, Gardiner SM and Bennett T (1989) Paraventricular nucleus injections of noradrenaline: cardiovascular effects in conscious Long-Evans and Brattleboro rats. *Brain Res* **496**:14-24.

Ireland LM, Cain JC, Rotert G, Thomas S, Shoghi S, Hancock AA and Kerwin JF, Jr. (1997) [3H]R-terazosin binds selectively to alpha1-adrenoceptors over alpha2-adrenoceptors - comparison with racemic [3H]terazosin and [3H]prazosin. *Eur J Pharmacol* **327**:79-86.

Kannan H, Hayashida Y and Yamashita H (1989) Increase in sympathetic outflow by paraventricular nucleus stimulation in awake rats. *Am J Physiol* **256**:R1325-1330.

Khawaled R, Bruening-Wright A, Adelman JP and Maylie J (1999) Bicuculline block of small-conductance calcium-activated potassium channels. *Pflugers Arch* **438**:314-321.

Li DP, Atnip LM, Chen SR and Pan HL (2005) Regulation of synaptic inputs to paraventricular-spinal output neurons by alpha2 adrenergic receptors. *J Neurophysiol* **93**:393-402.

Li DP, Chen SR and Pan HL (2002) Nitric oxide inhibits spinally projecting paraventricular neurons through potentiation of presynaptic GABA release. *J Neurophysiol* **88**:2664-2674.

Li DP, Chen SR and Pan HL (2003) Angiotensin II stimulates spinally projecting paraventricular neurons through presynaptic disinhibition. *J Neurosci* **23**:5041-5049.

Martin DS and Haywood JR (1993) Hemodynamic responses to paraventricular nucleus disinhibition with bicuculline in conscious rats. *Am J Physiol* **265**:H1727-1733.

Medgett IC and Langer SZ (1984) Heterogeneity of smooth muscle alpha adrenoceptors in rat tail artery in vitro. *J Pharmacol Exp Ther* **229**:823-830.

Perez DM, DeYoung MB and Graham RM (1993) Coupling of expressed alpha 1B- and alpha

1D-adrenergic receptor to multiple signaling pathways is both G protein and cell type specific. *Mol Pharmacol* **44**:784-795.

Plotsky PM (1987) Facilitation of immunoreactive corticotropin-releasing factor secretion into the hypophysial-portal circulation after activation of catecholaminergic pathways or central norepinephrine injection. *Endocrinology* **121**:924-930.

Pudovkina OL, Kawahara Y, de Vries J and Westerink BH (2001) The release of noradrenaline in the locus coeruleus and prefrontal cortex studied with dual-probe microdialysis. *Brain Res* **906**:38-45.

Pyner S and Coote JH (2000) Identification of branching paraventricular neurons of the hypothalamus that project to the rostroventrolateral medulla and spinal cord. *Neuroscience* **100**:549-556.

Qualy JM and Westfall TC (1988) Release of norepinephrine from the paraventricular hypothalamic nucleus of hypertensive rats. *Am J Physiol* **254**:H993-1003.

Sands SA and Morilak DA (1999) Expression of alpha1D adrenergic receptor messenger RNA in oxytocin- and corticotropin-releasing hormone-synthesizing neurons in the rat paraventricular nucleus. *Neuroscience* **91**:639-649.

Shafton AD, Ryan A and Badoer E (1998) Neurons in the hypothalamic paraventricular nucleus send collaterals to the spinal cord and to the rostral ventrolateral medulla in the rat. *Brain Res* **801**:239-243.

Swanson LW and Sawchenko PE (1983) Hypothalamic integration: organization of the paraventricular and supraoptic nuclei. *Annu Rev Neurosci* **6**:269-324.

Tasker JG and Dudek FE (1993) Local inhibitory synaptic inputs to neurones of the

paraventricular nucleus in slices of rat hypothalamus. *J Physiol* **469**:179-192.

Woo ND, Mukherjee K and Ganguly PK (1993) Norepinephrine levels in paraventricular nucleus of spontaneously hypertensive rats: role of neuropeptide Y. *Am J Physiol* **265**:H893-898.

Zahner MR and Pan HL (2005) Role of paraventricular nucleus in the cardiogenic sympathetic reflex in rats. *Am J Physiol Regul Integr Comp Physiol* **288**:R420-426.

Zhang K, Li YF and Patel KP (2002a) Reduced endogenous GABA-mediated inhibition in the PVN on renal nerve discharge in rats with heart failure. *Am J Physiol Regul Integr Comp Physiol* **282**:R1006-1015.

Zhang ZH, Francis J, Weiss RM and Felder RB (2002b) The renin-angiotensin-aldosterone system excites hypothalamic paraventricular nucleus neurons in heart failure. *Am J Physiol Heart Circ Physiol* **283**:H423-433.

Footnotes

This study was supported by grants from HL60026 and HL77400. The authors thank C.Y. Yang and P. Myers for technical assistance.

Figure Legends

Fig. 1. Effect of phenylephrine on the frequency of sEPSCs in labeled PVN neurons. *A*: original recordings showing sEPSCs during control, application of 10, 50 and 100 μM phenylephrine, washout, and perfusion of 20 μM CNQX in a labeled PVN neuron. *B*: cumulative probability plot of the same neuron showing the distribution of inter-event interval and amplitude of sEPSCs during control, perfusion of 50 and 100 μM phenylephrine, and washout. *C*: summary data showing effect of phenylephrine on the frequency and amplitude of sEPSCs (n = 19). Data are presented as means ± SEM. * $P < 0.05$, compared with the control (Kruskal-Wallis ANOVA followed by Dunn's post hoc test). phe, phenylephrine.

Fig. 2. Effect of corynanthine and prazosin on phenylephrine-induced increase in sEPSCs. *A*: raw tracings showing sEPSCs during control, perfusion of 50 μM phenylephrine, washout and perfusion of 50 μM phenylephrine plus 100 μM corynanthine in a labeled PVN neuron. *B*: cumulative probability plot showing the distribution of inter-event interval and amplitude of sEPSCs of the same neuron during control, perfusion of 50 μM phenylephrine, washout, and perfusion of 50 μM phenylephrine plus 100 μM corynanthine. *C*: summary data showing the effect of 100 μM corynanthine on phenylephrine-induced increase in sEPSCs (n = 11). *D*: summary data showing the effect of 20 μM prazosin on phenylephrine-induced increase in sEPSCs (n = 9). Data are presented as means ± SEM. * $P < 0.05$, compared with the control (Kruskal-Wallis ANOVA followed by Dunn's post hoc test). phe, phenylephrine; cory, corynanthine; prz, prazosin.

Fig. 3. Effect of phenylephrine on the frequency of sIPSCs and mEPSCs in labeled PVN neurons. *A*: raw tracings showing mEPSCs during control, perfusion of 50 μM phenylephrine and washout in a labeled PVN neuron. *B*: cumulative distribution probability plot of mEPSCs of the same neuron showing the distribution of inter-event interval and amplitude during control, perfusion of 50 μM phenylephrine, and washout. *C*: superimposed averages of 100 consecutive mEPSCs obtained between control and perfusion of 50 μM phenylephrine. The decay phase of mEPSCs was best fitted with a single exponential function. The decay time constant was similar in control (τ = 5.87 ms) and phenylephrine application (τ = 5.62 ms). *D*: summary data showing the effect of 50 μM phenylephrine on the frequency of mEPSCs in 13 labeled PVN neurons. Data are presented as means ± SEM. * $P < 0.05$, compared with the control; # $P < 0.05$, compared with the TTX treatment alone (Kruskal-Wallis ANOVA followed by Dunn's post hoc test). phe, phenylephrine.

Fig. 4. Effect of phenylephrine and cirazoline on the frequency of sIPSCs in labeled PVN neurons. *A*: raw tracings showing sIPSCs during control, application of 10, 50 and 100 μM phenylephrine, washout, and perfusion of 20 μM bicuculline in a labeled PVN neuron. *B*: cumulative probability plot of sIPSCs of the same neuron showing the distribution of inter-event interval and amplitude during control, perfusion of 50 and 100 μM phenylephrine, and washout. *C*: summary data showing the effect of 1-100 μM phenylephrine on the frequency and amplitude of sIPSCs (n = 13). *D*: summary data showing the effect of 1-100 μM cirazoline on the frequency of sIPSCs (n = 7). Data are presented as means ± SEM. * $P < 0.05$, compared with

the control (Kruskal-Wallis ANOVA followed by Dunn's post hoc test). phe, phenylephrine; Bic, bicuculline.

Fig. 5. Effect of corynanthine on the phenylephrine-induced decrease in sIPSCs. *A*: raw tracings showing control, perfusion of 50 μM phenylephrine, washout, and perfusion of 50 μM phenylephrine plus 100 μM corynanthine in a labeled PVN neuron. *B*: cumulative probability plot of sIPSCs of the same neuron showing the distribution of inter-event interval and amplitude during control, perfusion of 50 μM phenylephrine, washout, and perfusion of 50 μM phenylephrine plus 100 μM corynanthine. *C*: summary data showing that 100 μM corynanthine completely blocked the phenylephrine-induced decrease in the frequency of sIPSCs (n = 9). Data are presented as means ± SEM. * $P < 0.05$, compared with the control (Kruskal-Wallis ANOVA followed by Dunn's post hoc test). phe, phenylephrine; cory, corynanthine.

Fig. 6. Effect of phenylephrine on the frequency of mIPSCs in labeled PVN neurons. *A*: raw tracings showing mIPSCs during control, perfusion of 50 μM phenylephrine and washout in a labeled PVN neuron. *B*: cumulative probability plot of mIPSCs of the same neuron showing the distribution of inter-event interval and amplitude during control, perfusion of 50 μM phenylephrine, and washout. *C*: superimposed averages of 100 consecutive mIPSCs obtained during control and perfusion of 50 μM phenylephrine. The decay phase of mIPSCs was best fitted with a double exponential function. The decay time constant was similar during control and phenylephrine application (τ_{fast}: 12.79 vs. 13.02 ms; τ_{slow}: 49.10 vs. 50.39 ms). *D*: summary data showing the effect of 50 μM phenylephrine on the frequency of mIPSCs (n = 13). Data are

presented as means ± SEM. * P < 0.05, compared with the control (Kruskal-Wallis ANOVA followed by Dunn's post hoc test). phe, phenylephrine.

Fig. 7. Effect of phenylephrine on the firing rate of labeled PVN neurons in the presence of synaptic blockade. A: original tracings showing action currents of a labeled PVN neuron during control, perfusion of 50 μM phenylephrine, washout, perfusion of 20 μM bicuculline plus 20 μM CNQX plus 20 μM AP5, and 50 μM phenylephrine in the presence of bicuculline, CNQX and AP5. *B*: summary data showing the effect of 50 μM phenylephrine on the firing rate of 11 labeled PVN neurons before and after application of bicuculline, CNQX and AP5. *C*: summary data showing the differential effect of 100 and 500 nM apamin and 20 μM bicuculline on the firing activity of 8 labeled PVN neurons. Data are presented as means ± SEM. * P < 0.05, compared with the control (Kruskal-Wallis ANOVA followed by Dunn's post hoc test). phe, phenylephrine; Bic, bicuculline; apm, apamin.

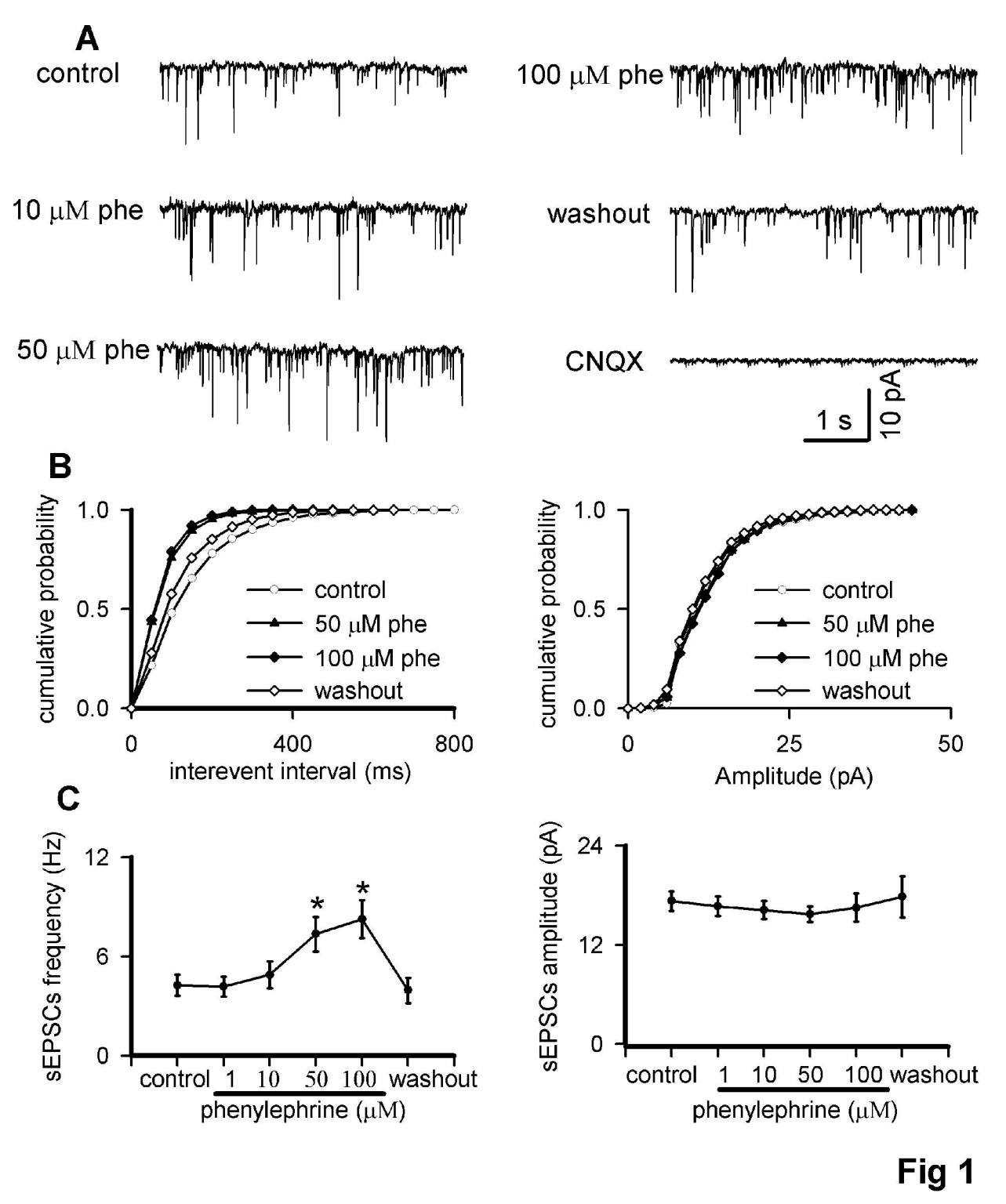
A
control
100 μM phe
10 μM phe
washout
50 μM phe
CNQX
1 s
10 pA
B
cumulative probability
1.0
0.5
0.0
0
400
800
interevent interval (ms)
control
50 μM phe
100 μM phe
washout
cumulative probability
1.0
0.5
0.0
0
25
50
Amplitude (pA)
control
50 μM phe
100 μM phe
washout
C
sEPSCs frequency (Hz)
12
6
0
*
*
control
1
10
50
100
washout
phenylephrine (μM)
sEPSCs amplitude (pA)
24
12
0
control
1
10
50
100
washout
phenylephrine (μM)

Fig 1

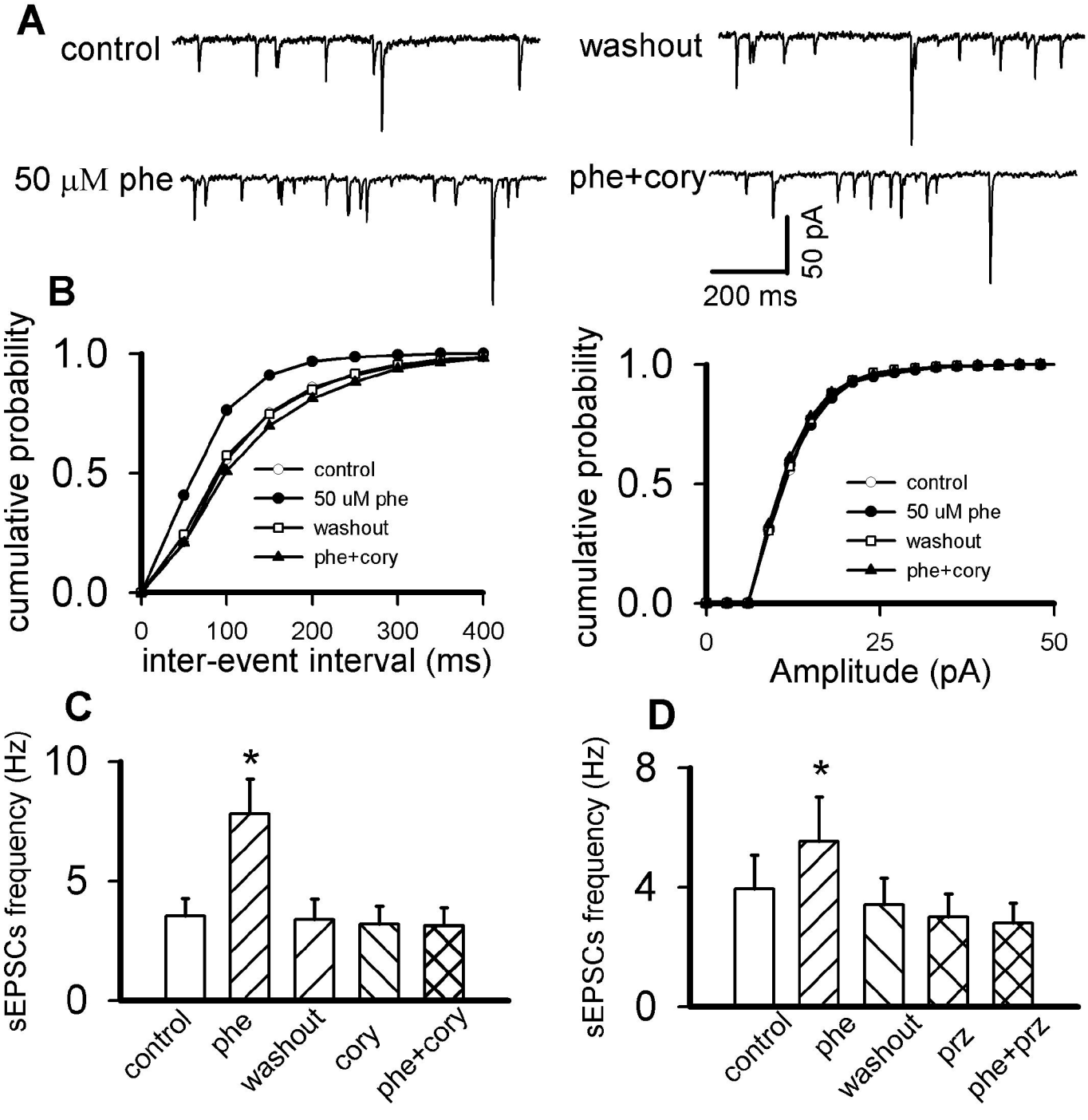
A
control
washout
50 μM phe
phe+cory
50 pA
200 ms
B
cumulative probability
1.0
0.5
0.0
0
100
200
300
400
inter-event interval (ms)
control
50 uM phe
washout
phe+cory
cumulative probability
1.0
0.5
0.0
0
25
50
Amplitude (pA)
control
50 uM phe
washout
phe+cory
C
sEPSCs frequency (Hz)
10
5
0
*
control
phe
washout
cory
phe+cory
D
sEPSCs frequency (Hz)
8
4
0
*
control
phe
washout
prz
phe+prz

Fig 2

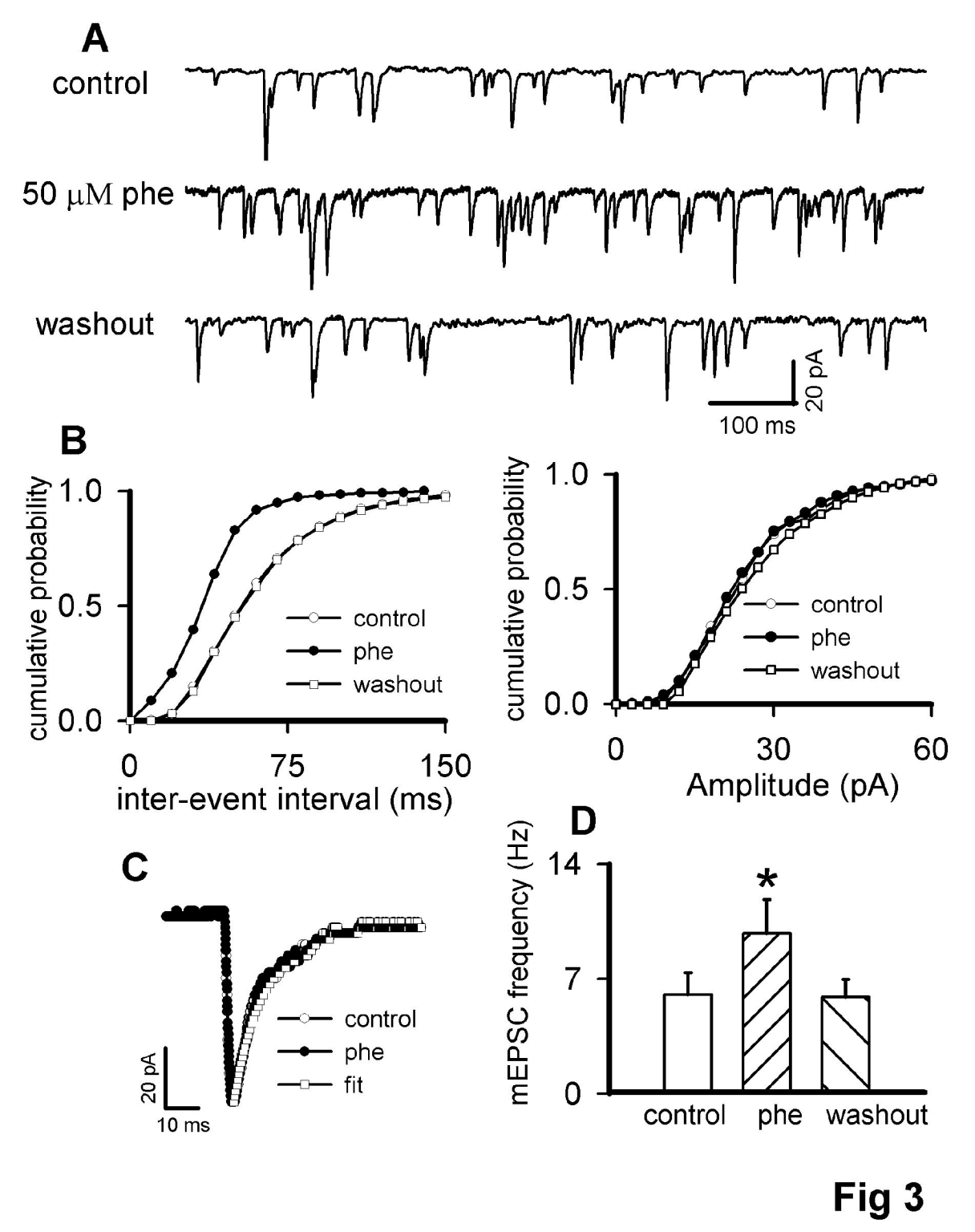
A
control
50 μM phe
washout
20 pA
100 ms
B
cumulative probability
1.0
0.5
0.0
0
75
150
inter-event interval (ms)
control
phe
washout
cumulative probability
1.0
0.5
0.0
0
30
60
Amplitude (pA)
control
phe
washout
C
20 pA
10 ms
control
phe
fit
D
mEPSC frequency (Hz)
14
7
0
*
control
phe
washout

Fig 3

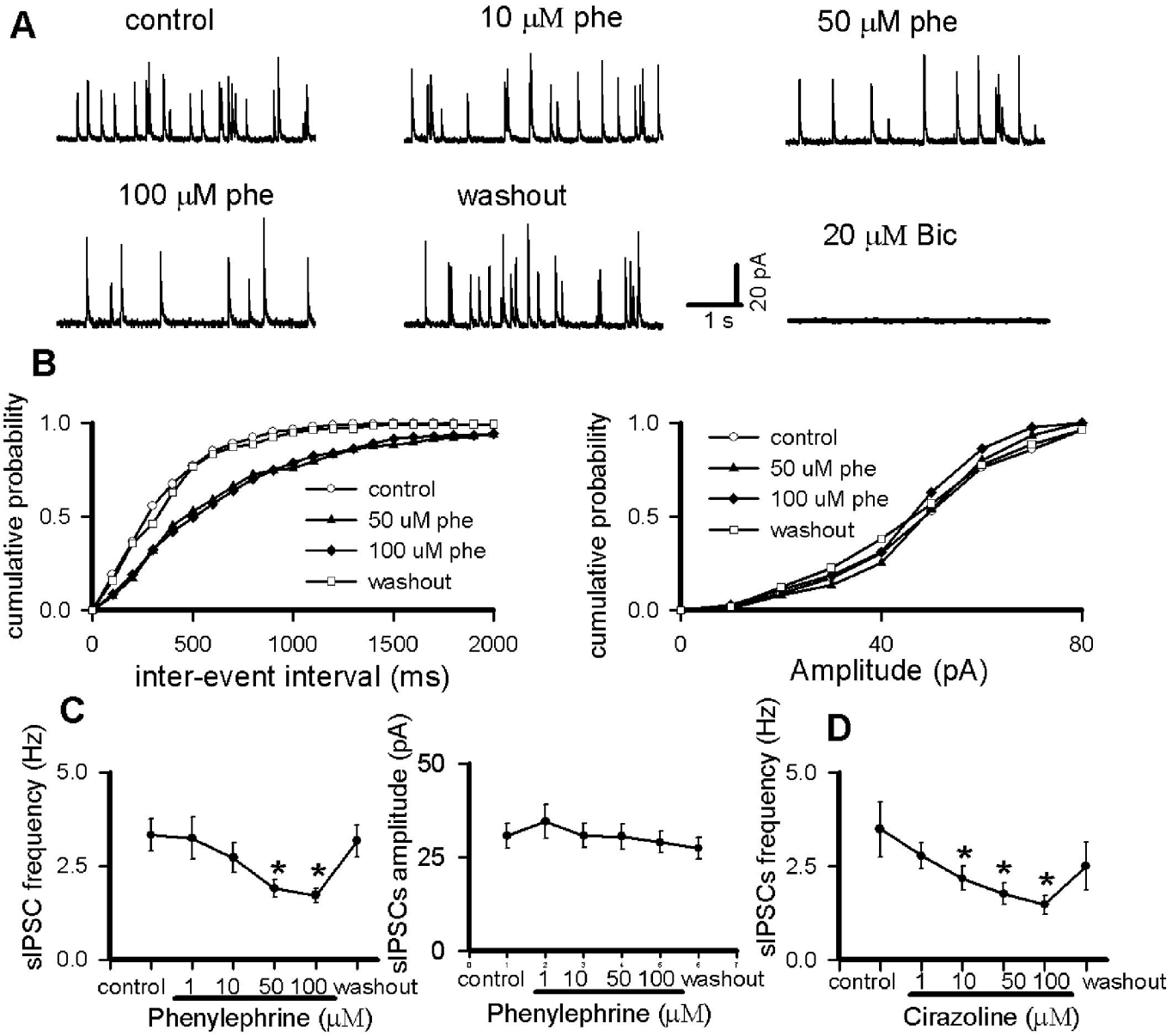
A
control
10 μM phe
50 μM phe
100 μM phe
washout
20 μM Bic
20 pA
1 s
B
cumulative probability
1.0
0.5
0.0
0
500
1000
1500
2000
inter-event interval (ms)
control
50 uM phe
100 uM phe
washout
cumulative probability
1.0
0.5
0.0
0
40
80
Amplitude (pA)
control
50 uM phe
100 uM phe
washout
C
sIPSC frequency (Hz)
5.0
2.5
0.0
control
1
10
50
100
washout
Phenylephrine (μM)
sIPSCs amplitude (pA)
50
25
0
control
1
10
50
100
washout
Phenylephrine (μM)
D
sIPSCs frequency (Hz)
5.0
2.5
0.0
control
1
10
50
100
washout
Cirazoline (μM)

Fig 4

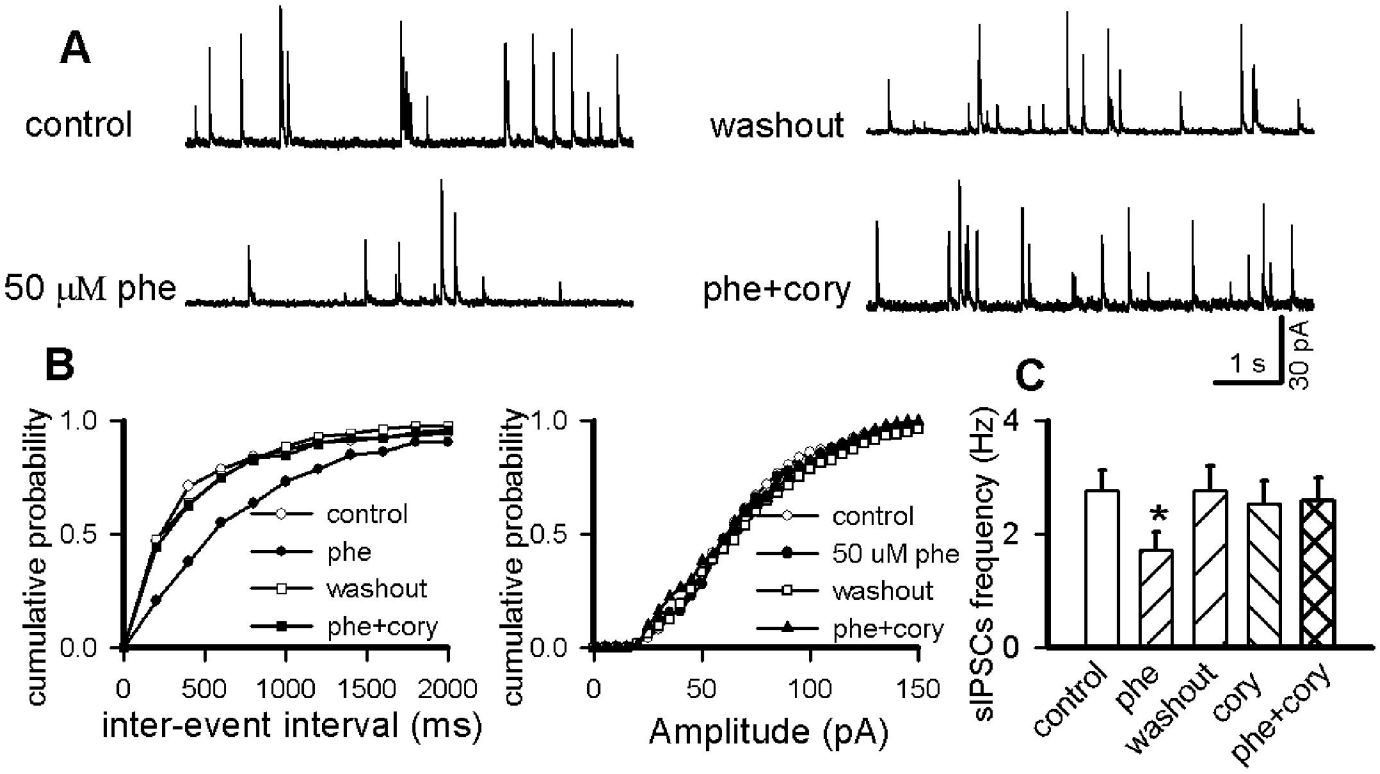
A
control
washout
50 μM phe
phe+cory
1 s
30 pA
B
cumulative probability
1.0
0.5
0.0
0
500
1000
1500
2000
inter-event interval (ms)
control
phe
washout
phe+cory
cumulative probability
1.0
0.5
0.0
0
50
100
150
Amplitude (pA)
control
50 uM phe
washout
phe+cory
C
sIPSCs frequency (Hz)
4
2
0
*
control
phe
washout
cory
phe+cory

Fig 5

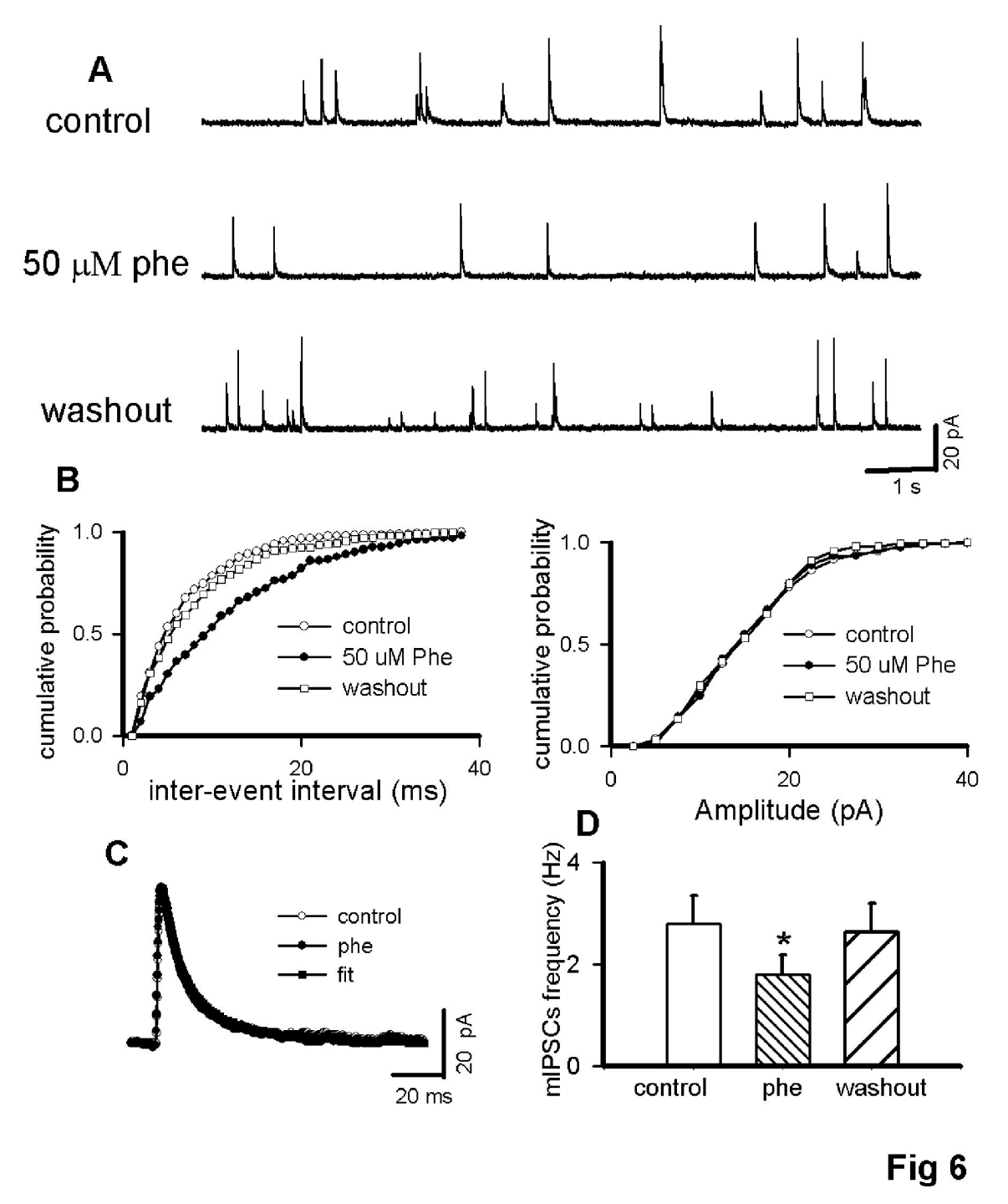
A
control
50 μM phe
washout
20 pA
1 s
B
cumulative probability
1.0
0.5
0.0
0
20
40
inter-event interval (ms)
control
50 uM Phe
washout
cumulative probability
1.0
0.5
0.0
0
20
40
Amplitude (pA)
control
50 uM Phe
washout
C
control
phe
fit
20 pA
20 ms
D
mIPSCs frequency (Hz)
4
2
0
*
control
phe
washout

Fig 6

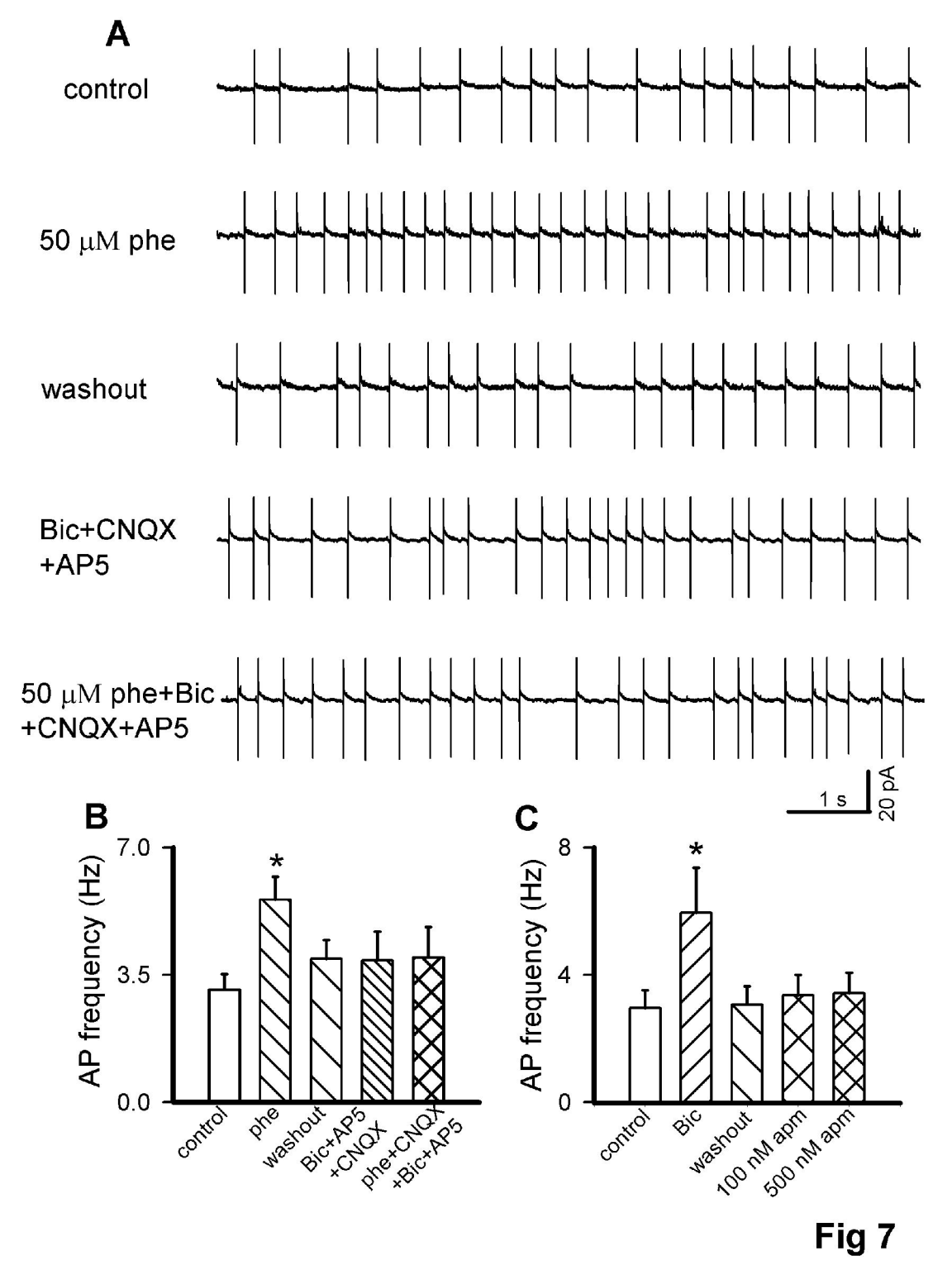
A
control
50 μM phe
washout
Bic+CNQX
+AP5
50 μM phe+Bic
+CNQX+AP5
1 s
20 pA
B
AP frequency (Hz)
7.0
3.5
0.0
*
control
phe
washout
Bic+AP5
+CNQX
phe+CNQX
+Bic+AP5
C
AP frequency (Hz)
8
4
0
*
control
Bic
washout
100 nM apm
500 nM apm

Fig 7